Static and aeroelastic limit states of "Ponte della Musica" via a fully nonlinear continuum model

Andrea Arena[1], Walter Lacarbonara[1]
[1]*Department of Structural and Geotechnical Engineering, University of Rome "La Sapienza", Italy*
E-mail: andrea.arena@uniroma1.it, walter.lacarbonara@uniroma1.it

Keywords: Arch bridge, wind flutter condition, flexural-torsional coupling, geometrically exact approach.

SUMMARY. A parametric three-dimensional model of an arch bridge under fairly general static and dynamic loading conditions is proposed. The arch bridge geometry is parameterized in such a way that it also allows to account for generic inclinations of the arches with respect to the vertical configuration. By employing an exact kinematic formulation, the strain parameters are expressed as nonlinear functions of the displacement gradients and all deformation modes are considered, including shear, torsional and out-of-plane bending modes, both in the deck and supporting arches. The nonlinear equations of motion are obtained via a direct total Lagrangian formulation by adopting linearly hyperelastic constitutive equations for all structural members. The parametric nonlinear model, constructed for the specific case of *Ponte della Musica* in Rome, is employed to investigate the limit states appearing either as a limit point through path-following the response along the prescribed loading path or as the critical condition of a suitable eigenvalue problem associated with the equations of motion linearized about the in-service pre-stressed bridge configuration subject to the dead loads and wind forces. The proposed model takes into account the fully nonlinear extensional-flexural-torsional coupling and examines the aeroelastic effects induced by the wind forces with special attention to the calculation of the flutter speed and critical flutter mode shape.

1 INTRODUCTION

Arch bridges are peculiar structures that exhibit a nonlinear pre-critical behavior under the action of quasi-static incremental loads. When these loads are such that they induce an increase of the compressional stresses in the arches, a significant loss of stiffness is suffered by the arches due to the negative geometric stiffness contribution. Various numerical models of arch bridges have been proposed in the technical literature and different studies have been performed to investigate the elastic instability of this kind of structures. Wen and Medallah [1] and Nazmy [2] used the linear buckling method for the evaluation of the ultimate load multiplier of steel arch bridges; this kind of approach does not allow to evaluate the pre-critical behavior as well as the loss of stiffness induced by incremental compressive loads. A nonlinear buckling approach, based on geometric and material nonlinearities, has been proposed by Komatsu and Sakimoto [3] to investigate the buckling limite state of steel arches. They proposed a three-dimensional analytical model based on elasto-plastic constitutive equations and on small-strain finite kinematics; moreover, they enforced the unshearability constraint of the arch cross sections.

The here proposed continuum model allows to consider more generic arches geometries (e.g., inclined arches) and to investigate the nonlinear behavior of the arch-deck system by incremental parametric analysis. The accurate evaluation of the tangent stiffness in the bridge pre-stressed condition induced by the in-service loads is an important step of a more accurate study of the wind-structure interaction and the associated limit states such as flutter or torsional divergence. Moreover, also the torsional and the out-of-plane components of the motion are necessary to describe accu-

rately the bridge response to aeroelastic forces. Thus the proposed three-dimensional fully nonlinear model becomes a suitable parametric framework to investigate the mentioned limit states in arch bridges allowing at the same time efficient structural optimization studies.

To investigate the aeroelastic phenomenon induced by the static component of the wind action, a three-dimensional continuum model of a suspension bridge was proposed by Lacarbonara and Arena [4, 5]. The model was formulated via a total Lagrangian approach whereby finite kinematics and large strains were assumed. The torsional divergence was determined as the singularity condition in the tangent stiffness obtained by path-following the nonlinear equilibrium response for an increasing static wind action.

On the other hand, the flutter instability phenomenon is classically studied by using two different approaches. Simiu and Scanlan [6] proposed to evaluate the critical wind velocity by solving an eigenvalue problem whose solution represents the coupled flexural-torsional natural frequency at the flutter condition. An alternative strategy is to perform a time-domain analysis of the bridge response in a certain range of wind speeds (see for example [7]); the critical condition is attained when a harmonic motion of the structure is obtained. In both procedures, the aerodynamic forces are modelled using the so-called aeroelastic derivatives, that correspond to a set of functions evaluated through wind-tunnel tests on a sectional scaled model of the reference bridge [8]. In the proposed work, the eigenvalue approach has been pursued and the characteristic complex-valued eigenvalue problem has been defined for a continuum three-dimensional model to take into account the global structural stiffness and mass.

The reference structure is the arch bridge named *Ponte della Musica*, architecturally designed by Buro Happold Consulting Engineers in association with Powell-Williams Architects, and structurally designed by Prof. M.P. Petrangeli and Associates. The bridge is currently under construction on the Tiber river in Rome. Its peculiarity lies in the fact that the arches are inclined with respect to the vertical planes so that the global torsional stiffness of the bridge turns out to be lower with respect to the more usual vertical arch bridge geometries. Moreover, the deck is fairly large and slender and the arches thrusts are transferred to the deck using a sophisticated constraining mechanism at the boundary designed by M.P. Petrangeli and Associates [9].

2 NONLINEAR CONTINUUM MODEL AND EQUATIONS OF MOTION

The three-dimensional parametric model is based on a kinematically exact approach while the equations of motion are obtained within the context of a total Lagrangian formulation. In the orthonormal basis of a fixed inertial reference frame $(\boldsymbol{i}_1, \boldsymbol{i}_2, \boldsymbol{i}_3)$, with the origin in the center of mass of the left deck terminal cross section, the reference stress-free configuration of each arch is described by the position vectors $\boldsymbol{x}^{\pm}(x) = x\ \boldsymbol{i}_1^{\pm} + y(x)\cos\alpha^{\pm}\boldsymbol{i}_2^{\pm} + y(x)\sin\alpha^{\pm}\boldsymbol{i}_3^{\pm}$, where x is the reference coordinate collinear with $\boldsymbol{i}_1$ (see Figure 1); $y(x)$ describes the parabolic shape of the arch centerline in a vertical (unrotated) plane and $\alpha^{\pm}$ represents the arch inclination angle with respect to the vertical plane (with $\alpha^{\pm} = \pm\alpha$). The superscripts "+" and "-" denote the two arches, the plus refers to the arch undergoing incremental compression, the minus to that subject to compression loosening, respectively, when the deck suffers a counterclockwise rotation about $\boldsymbol{i}_1$. Further, the current configuration of the cross sections is described by the unit vectors $\left(\boldsymbol{b}_1^{\pm}, \boldsymbol{b}_2^{\pm}, \boldsymbol{b}_3^{\pm}\right)$ that are obtained from the reference frame with the sequence of finite rotations expressed by the following matrices:

$$\mathbf{Q}^{\pm} = \begin{bmatrix} 1 & 0 & 0 \\ 0 & \cos\alpha^{\pm} & -\sin\alpha^{\pm} \\ 0 & \sin\alpha^{\pm} & \cos\alpha^{\pm} \end{bmatrix}, \quad \mathbf{Q}^{0}(x) = \begin{bmatrix} \cos\theta(x) & -\sin\theta(x) & 0 \\ \sin\theta(x) & \cos\theta(x) & 0 \\ 0 & 0 & 1 \end{bmatrix}, \tag{1}$$

$$\mathbf{R}^{\pm} = \begin{bmatrix} \cos\phi_2\cos\phi_3 & \cos\phi_3\sin\phi_1\sin\phi_2 - \cos\phi_1\sin\phi_3 & \cos\phi_1\cos\phi_3\sin\phi_2 + \sin\phi_1\sin\phi_3 \\ \cos\phi_2\sin\phi_3 & \cos\phi_1\cos\phi_3 + \sin\phi_1\sin\phi_2\sin\phi_3 & \cos\phi_1\sin\phi_2\sin\phi_3 - \cos\phi_3\sin\phi_1 \\ -\sin\phi_2 & \cos\phi_2\sin\phi_1 & \cos\phi_1\cos\phi_2 \end{bmatrix},$$

where matrices $\mathbf{Q}^{\pm}$ represent the rotations $(\pm\alpha)$ about $\boldsymbol{i}_1$ of the planes containing the arches and $\mathbf{Q}^0(x)$ defines the cross-sections local basis rotation along the undeformed arc-length in the inclined reference planes with $\theta(x) = \arctan[dy/dx]$. Orthogonal tensor $\mathbf{R}^{\pm}(x,t)$ represents the finite rotations undergone by the arches local bases during the motion, superscripts $\pm$ of rotations ϕ_i have been dropped for the sake of notational conciseness; similarly, $\mathbf{R}(x,t)$ will be used to describe the finite rotations of the deck local basis $(\boldsymbol{b}_1, \boldsymbol{b}_2, \boldsymbol{b}_3)$.

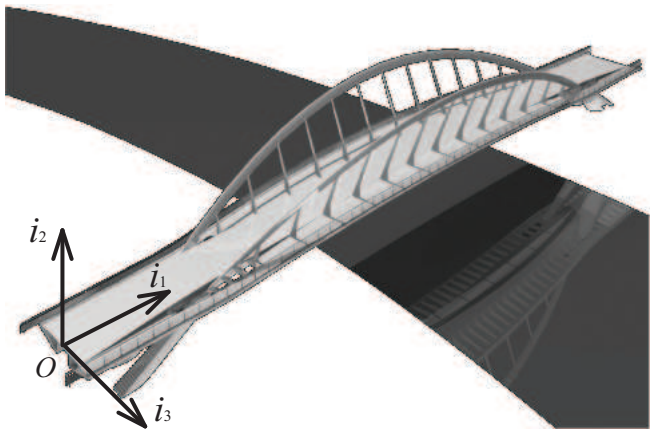

Figure 1: Three-dimensional view of *Ponte della Musica*.

In the actual configuration, the deck and arches local bases can thus be obtained from the inertial reference frame $(\boldsymbol{i}_1, \boldsymbol{i}_2, \boldsymbol{i}_3)$ as:

$$\begin{bmatrix} \boldsymbol{b}_1(x,t) \\ \boldsymbol{b}_2(x,t) \\ \boldsymbol{b}_3(x,t) \end{bmatrix} = \mathbf{R}^{\top}(x,t) \begin{bmatrix} \boldsymbol{i}_1 \\ \boldsymbol{i}_2 \\ \boldsymbol{i}_3 \end{bmatrix}, \quad \begin{bmatrix} \boldsymbol{b}_1^{\pm}(x,t) \\ \boldsymbol{b}_2^{\pm}(x,t) \\ \boldsymbol{b}_3^{\pm}(x,t) \end{bmatrix} = \left(\mathbf{Q}^{\pm}\cdot\mathbf{Q}^0(x)\cdot\mathbf{R}^{\pm}(x,t)\right)^{\top} \begin{bmatrix} \boldsymbol{i}_1 \\ \boldsymbol{i}_2 \\ \boldsymbol{i}_3 \end{bmatrix} \quad (2)$$

where the superscript $\top$ indicates the transpose. The position vectors of the base curves of the arches in the actual configuration are defined as

$$\boldsymbol{r}^{\pm}(x,t) = \left[x + v_1^{\pm}(x,t)\right]\boldsymbol{i}_1 + [y(x)\cos\alpha^{\pm} + v_2^{\pm}(x,t)]\boldsymbol{i}_2 + [y(x)\sin\alpha^{\pm} + v_3^{\pm}(x,t)]\boldsymbol{i}_3. \quad (3)$$

The arches finite strain and curvature vectors are given by [10]

$$\boldsymbol{\epsilon}^{\pm} = \left(\nu^{\pm} - 1\right)\boldsymbol{b}_1^{\pm} + \eta_2^{\pm}\boldsymbol{b}_2^{\pm} + \eta_3^{\pm}\boldsymbol{b}_3^{\pm}, \quad \text{and} \quad \boldsymbol{\mu}^{\pm} = \mu_1^{\pm}\boldsymbol{b}_1^{\pm} + \mu_2^{\pm}\boldsymbol{b}_2^{\pm} + \mu_3^{\pm}\boldsymbol{b}_3^{\pm}.$$

The components of $\boldsymbol{\epsilon}^{\pm}$ and $\boldsymbol{\mu}^{\pm}$ are the arches strain variables. In particular, the components of $\boldsymbol{\epsilon}^{\pm}$ are the arch elongation and the shear strains in the two local directions, respectively, whereas the components of $\boldsymbol{\mu}^{\pm}$ are the bending curvatures about the two local axes and the torsional curvature.

They are explicitly obtained through the following expressions:

$$\begin{aligned}
&\nu^{\pm} = \frac{d\boldsymbol{r}^{\pm}}{ds} \cdot \boldsymbol{b}_1^{\pm} \ , \ \eta_2^{\pm} = \frac{d\boldsymbol{r}^{\pm}}{ds} \cdot \boldsymbol{b}_2^{\pm} \ , \ \eta_3^{\pm} = \frac{d\boldsymbol{r}^{\pm}}{ds} \cdot \boldsymbol{b}_3^{\pm} \\
&\frac{d\boldsymbol{b}_k^{\pm}}{ds} = \boldsymbol{\mu}^{\pm} \times \boldsymbol{b}_k^{\pm} + \mathbf{R}^{\pm} \cdot \boldsymbol{\mu}_0^{\pm} \times \boldsymbol{b}_{k,0}^{\pm} = \breve{\boldsymbol{\mu}}^{\pm} \times \boldsymbol{b}_k^{\pm} \ , \quad \forall\, k = 1,2,3.
\end{aligned} \tag{4}$$

where s is the arc-length along the centerlines of the undeformed arches. By employing the same approach, we set up the parameters describing the finite kinematics of the bridge deck. In particular, the position vector of the centerline is $\boldsymbol{r}(x,t) = \boldsymbol{x}(x) + \boldsymbol{u}(x,t)$, and the strain and curvature vectors are obtained as $\boldsymbol{\epsilon} = \mathbf{R}^{\top} \cdot \boldsymbol{r}' - \boldsymbol{x}'$, $\boldsymbol{\mu} = \mathbf{R}^{\top} \cdot \mathbf{R}'$, where $(\cdot)'$ indicates differentiation with respect to x. The equations of motion, obtained by enforcing the balance of linear and angular momentum for the arch-deck system, are expressed as

$$\begin{aligned}
\partial_x \boldsymbol{n}^{\pm}(x,t) + \boldsymbol{f}^{\pm}(x,t) + \boldsymbol{h}_j^{\pm}(x,t) &= (\rho A)^a \sec\theta \ \ddot{\boldsymbol{v}}^{\pm} \\
\partial_x \boldsymbol{m}^{\pm}(x,t) + \partial_x \boldsymbol{r}^{\pm}(x,t) \times \boldsymbol{n}^{\pm}(x,t) + \boldsymbol{c}^{\pm}(x,t) + \boldsymbol{c}_j^{\pm}(x,t) &= (\rho J_1)^a \sec\theta \ \ddot{\phi}_1^{\pm} \boldsymbol{i}_1 \\
\partial_x \boldsymbol{n}(x,t) + \boldsymbol{f}(x,t) + \boldsymbol{h}_i^{+}(x,t) + \boldsymbol{h}_i^{-}(x,t) &= (\rho A)^b \ \ddot{\boldsymbol{u}} \\
\partial_x \boldsymbol{m}(x,t) + \partial_x \boldsymbol{r}(x,t) \times \boldsymbol{n}(x,t) + B\boldsymbol{b}_3 \times \left(\boldsymbol{h}_i^{+}(x,t) - \boldsymbol{h}_i^{-}(x,t)\right) + \left(\boldsymbol{c}_i^{+}(x,t) + \boldsymbol{c}_i^{-}(x,t)\right) & \\
+\boldsymbol{c}(x,t) = (\rho J_1)^b \ddot{\phi}_1 \boldsymbol{i}_1 &
\end{aligned} \tag{5}$$

where $\partial_x(\cdot)$ indicates partial differentiation with respect to x while the overdot denotes differentiation with respect to time t. Vectors $(\boldsymbol{n}^{\pm},\ \boldsymbol{m}^{\pm})$ and $(\boldsymbol{n},\ \boldsymbol{m})$ represent the contact forces and couples for the arches and the deck, respectively. Moreover, $(\boldsymbol{f}^{\pm},\ \boldsymbol{c}^{\pm})$ and $(\boldsymbol{f},\ \boldsymbol{c})$ are the external forces and couples per unit reference length acting on the structural members.

The connections between the arches and the deck are modelled as three-dimensional Euler-Bernoulli beams whose nodal forces and couples, expressed in terms of the nodal displacements and rotations, are assumed applied on the bridge span as δ-Dirac functions centered at the considered hanger position x_p. That is,

$$\begin{aligned}
\boldsymbol{h}_i^{\pm}(x,t) &= \sum_{p=1}^{N_p} \delta\left(x - x_p\right) \boldsymbol{h}_{p,i}^{\pm}(t) \ , \quad \boldsymbol{h}_j^{\pm}(x,t) = \sum_{p=1}^{N_p} \delta\left(x - x_p\right) \boldsymbol{h}_{p,j}^{\pm}(t) \\
\boldsymbol{c}_i^{\pm}(x,t) &= \sum_{p=1}^{N_p} \delta\left(x - x_p\right) \boldsymbol{c}_{p,i}^{\pm}(t) \ , \quad \boldsymbol{c}_j^{\pm}(x,t) = \sum_{p=1}^{N_p} \delta\left(x - x_p\right) \boldsymbol{c}_{p,j}^{\pm}(t)
\end{aligned} \tag{6}$$

We assume that node i is on the deck and node j is on the arch, N_p is the total number of hangers by side. By denoting $\mathbf{F}_p^{\pm} = \left[\ \boldsymbol{h}_{p,i}^{\pm} \quad \boldsymbol{c}_{p,i}^{\pm} \quad \boldsymbol{h}_{p,j}^{\pm} \quad \boldsymbol{c}_{p,j}^{\pm}\ \right]^{\top}$ the vector collecting all hanger nodal forces and couples and $\mathbf{U}_p^{\pm} = \left[\ \boldsymbol{u}^{\pm} \quad \boldsymbol{\phi} \quad \boldsymbol{v}^{\pm} \quad \boldsymbol{\phi}^{\pm}\ \right]^{\top}$ the vector of nodal displacements and rotations, the condensed linear constitutive equations read $\mathbf{F}_p^{\pm} = \mathbf{K}_p \mathbf{U}_p^{\pm}$, where $\mathbf{K}_p$ is the linear stiffness matrix. The displacements of the deck points, to which the hangers are attached, are given by $\boldsymbol{u}^{\pm}(x,t) = \boldsymbol{u}(x,t) \mp d\left[\sin\phi_1 \boldsymbol{i}_2 + (1 - \cos\phi_1)\, \boldsymbol{i}_3\right]$ where d is the distance along $\boldsymbol{i}_3$ between the hangers attachment points and the deck centerline while ϕ_1 is the deck torsional rotation angle.

2.1 *Boundary conditions and computational approach*

The design of *Ponte della Musica* features two parabolic arches inclined by 15° with respect to the vertical plane and connected to the deck by twelve inclined steel beams. Furthermore, the arches

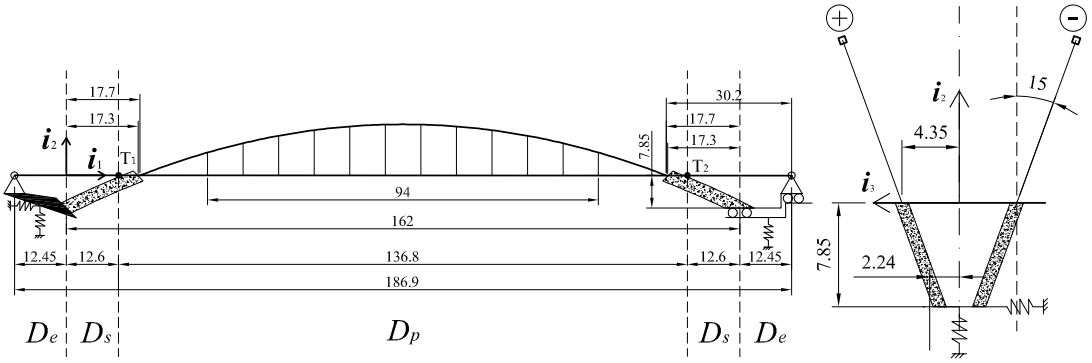

Figure 2: *Ponte della Musica*: structural scheme (lengths are expressed in meters).

are constrained to the deck at nodes T_1 and T_2 in the vertical and out-of-plane displacements, as shown in Figure 2. The arches are made of steel in the sections above the deck, otherwise they are made of reinforced concrete. The variation of the sectional properties is accounted for by modelling the arches elastic properties as a summation of Heaviside functions along the deck span.

At the boundaries, the structural elements are connected by reinforced concrete plates that ensure the transfer of the arches thrusts to the deck; each plate is built on piles which are modelled as equivalent translational springs of stiffness k in the three global directions $\boldsymbol{i}_1$, $\boldsymbol{i}_2$, and $\boldsymbol{i}_3$, respectively.

The vector-valued equations of motion (5), projected into the global basis $(\boldsymbol{i}_1, \boldsymbol{i}_2, \boldsymbol{i}_3)$, yield 18 nonlinear partial-differential equations in 18 independent kinematic unknowns. The obtained equations of motion govern the elastodynamic problem of the arch bridge. Such equations, as well as the boundary conditions, cast in a suitable nondimensional form, have been implemented and solved in PDE mode by the finite element computational platform *COMSOL Multiphysics*. The finite elements used for the analysis are *Lagrangian* quadratic elements and the degree of the mesh refinement has been adapted to optimize the accuracy and evaluation time of the solution.

3 STATIC STABILITY ANALYSIS

In the following the results of a static incremental analysis are discussed. The analysis is aimed at investigating the limit state corresponding to the loss of elastic stability of *Ponte della Musica* and at evaluating the static load multiplier at which the structure suffers the elastic instability. Load paths have been constructed starting from the bridge pre-stressed configuration due to self-weight and the other dead loads; an incremental load is applied by increasing the load multiplier λ of the accidental loads induced by vehicles and pedestrian. The incremental load is modelled according to the standard schemes defined by the European design codes (Eurocodes) [11, 12]. The worst loading scenario is represented, for the vehicles, by a three-point load distribution centered about the deck midspan and by two uniform distributions on the rest of the deck whereas, for the pedestrian-induced load, by a uniform distribution on the overall deck span. Both the vehicles and pedestrians are considered as simultaneous loads acting on the bridge.

As expected, the nonlinear softening load paths of the bridge are due to the arches that under compression suffer a stiffness degradation due to the induced negative geometric stiffness. Furthermore, these nonlinear effects become appreciable at low values of the load multiplier ($\lambda \approx 5 \div 6$) and the annihilation of the bridge global tangent stiffness is reached when $\lambda \approx 14 \div 15$, in agreement

with the results of previous structural analysis of the bridge [9].

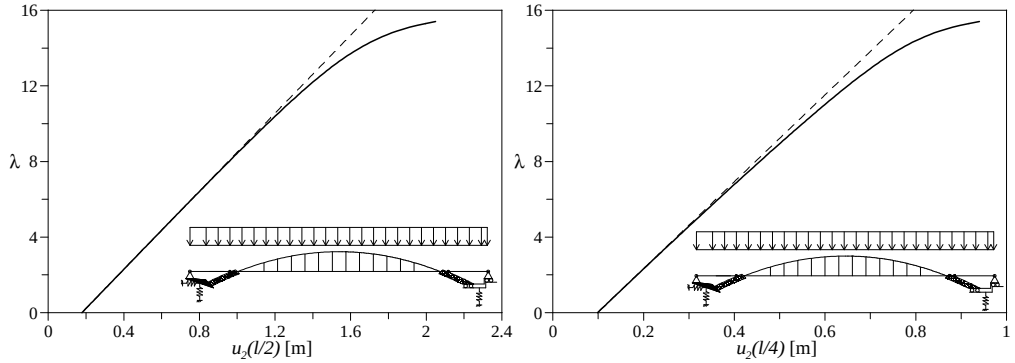

Figure 3: Nonlinear load paths: deck vertical displacements u_2 at $l/2$ and $l/4$. The dashed lines indicate the results of the linearized model, the solid lines denote the results of the fully nonlinear model.

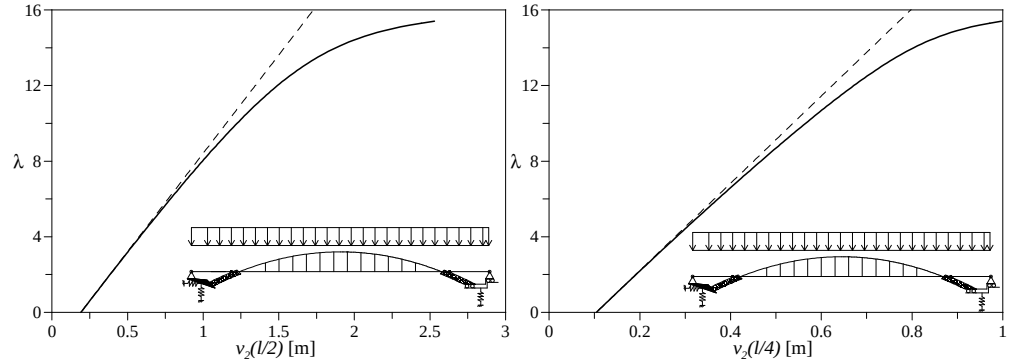

Figure 4: Nonlinear load paths: arches vertical displacements v_2 at $l/2$ and $l/4$. The dashed lines indicate the results of the linearized model, the solid lines denote the results of the fully nonlinear model.

4 FLUTTER ANALYSIS

An aeroelastic stability analysis has been carried out for the reference arch bridge with the aim of determining the critical wind velocity that induces the flutter condition. The study has been conducted by linearizing the equations of motion first about the stress-free configuration and, subsequently, about the in-service configuration so as to evaluate the effects of the lower global stiffness induced by the compressional pre-stress in the arches. By a preliminary modal analysis, the natural frequencies of the bridge and the associated mode shapes have been calculated; the results, for the lowest five modes, are summarized in Table 1.

	Mode 1 Flex-Tor *symm* $u_3, v_3^{\pm}, \phi_1, v_2^{\pm}$	Mode 2 Flex *skew* $u_2, v_2^{\pm}, (v_3^{\pm})$	Mode 3 Flex *symm* $u_2, v_2^{\pm}, (v_3^{\pm})$	Mode 4 Flex *symm* $u_2, v_2^{\pm}, (v_3^{\pm})$	Mode 5 Flex-Tor *symm* $u_3, v_3^{\pm}, \phi_1, v_2^{\pm}$
$T_i[s]$	1.37682	1.29931	1.10461	0.79299	0.73842
$f_i[Hz]$	0.726	0.770	0.905	1.261	1.354

Table 1: Lowest five periods and frequencies of *Ponte della Musica*.

The analysis results proposed in Table 1 are in good agreement with the values obtained by independent structural finite element models [9] and show how the first natural mode of the bridge is a coupled lateral flexural-torsional (u_3 , ϕ_1) vibration mode and the first flexural vertical mode (u_2) has its frequency near the torsional one. According to the technical literature about aerodynamic analysis [6, 8], only the lift force and the aerodynamic moment are considered as the leading bridge aerodynamic loads by considering negligible the effects induced by the drag forces. The following classical form of the aerodynamic loads is taken into account [6]:

$$\begin{aligned} f_2^A &= \frac{1}{2}\rho B U^2 \left(\frac{K}{U} H_1^* \dot{u}_2 + \frac{KB}{U} H_2^* \dot{\phi}_1 + K^2 H_3^* \phi_1 + \frac{K^2}{B} H_4^* u_2 \right) \\ c_1^A &= \frac{1}{2}\rho B^2 U^2 \left(\frac{K}{U} A_1^* \dot{u}_2 + \frac{KB}{U} A_2^* \dot{\phi}_1 + K^2 A_3^* \phi_1 + \frac{K^2}{B} A_4^* u_2 \right) \end{aligned} \tag{7}$$

Expressions (7) are substituted into equations of motion (5) as components of $\boldsymbol{f}(x,t)$ in the direction collinear with $\boldsymbol{i}_2$ and of $\boldsymbol{c}(x,t)$ in the $\boldsymbol{i}_1-$direction, respectively. In consonance with classical notations, ρ denotes the air density, B is the deck depth, U is the dimensional wind velocity, K the reduced frequency defined as $K = B\omega/U$ where ω is the circular flutter frequency.

Coefficients A_i^* and H_i^* are the flutter derivatives which have been experimentally determined through extensive wind tunnel tests at the CRIACIV laboratory in the town of Prato [14]. To evaluate the flutter velocity, the complex-valued eigenvalue problem governing the phenomenon is solved in a range of reduced wind velocity, $U_r = 2\pi U/(\omega B)$, so as to determine the critical condition at which a purely imaginary eigenvalue signals the onset of flutter. By introducing the nondimensional circular frequency σ, the solution of the dynamic problem is assumed in the form $\left(\boldsymbol{u}(x,t), \boldsymbol{\phi}(x,t), \boldsymbol{v}^{\pm}(x,t), \boldsymbol{\phi}^{\pm}(x,t)\right) = \left(\widetilde{\boldsymbol{u}}(x), \widetilde{\boldsymbol{\phi}}(x), \widetilde{\boldsymbol{v}}^{\pm}(x), \widetilde{\boldsymbol{\phi}}^{\pm}(x)\right) e^{i\sigma t}$. Accordingly, the flutter condition is obtained when the eigenvalue $\sigma = \sigma_R + i\sigma_I$ becomes purely real. The values of the aeroelastic derivatives were obtained for two different angles of attack, namely $\alpha = 0^\circ$ and $\alpha = +3^\circ$. Moreover, the limit state has been calculated considering both the undamped condition and the damped condition with $\zeta = 0.5\%$, a typical damping ratio for bridge structures.

The results obtained solving the eigenvalue problem, linearized about the bridge undeformed configuration, turned out to be in close agreement with the values of the flutter velocity experimentally measured in the wind tunnel tests; in particular, the difference is bounded between 1% and 5%. Furthermore, by accounting for the bridge pre-stressed state, we obtained a lower value of the flutter wind velocity, as expected. Table 2 summarizes most of the computational results compared with the experimental measurements. In the same table, $U_{r,c} > \overline{U}_r\,(= 16.3)$ indicates that the flutter condition is not reached in the given range of reduced velocity. Figure 7 portrays the critical flutter mode shape of *Ponte della Musica*, considering the modal components, separately, for the deck and the arches. The flutter mode shape for the deck is reminiscent of the fundamental mode with comparable contributions in the out-of-plane bending modal displacement u_3 and in the torsional component ϕ_1 with the addition of a small in-plane bending component u_2.

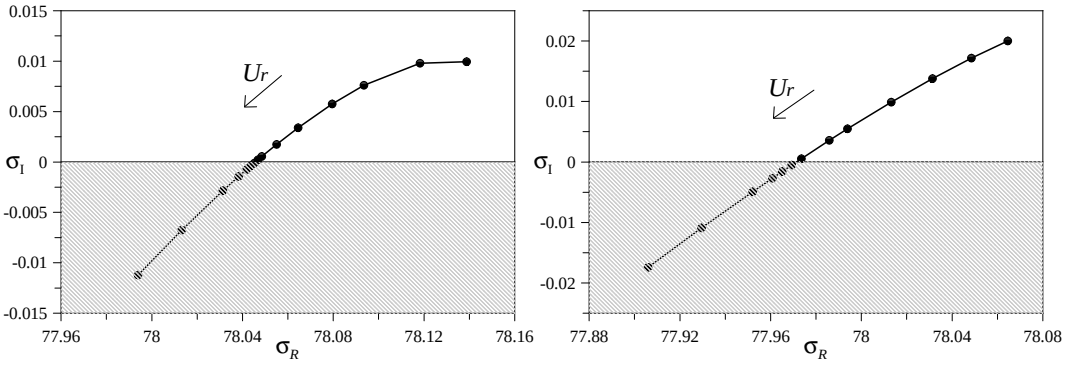

Figure 5: Flutter (grey zone) and stability (white zone) regions, undamped (left) and damped (right), when the wind angle of attack is $\alpha = +3^\circ$.

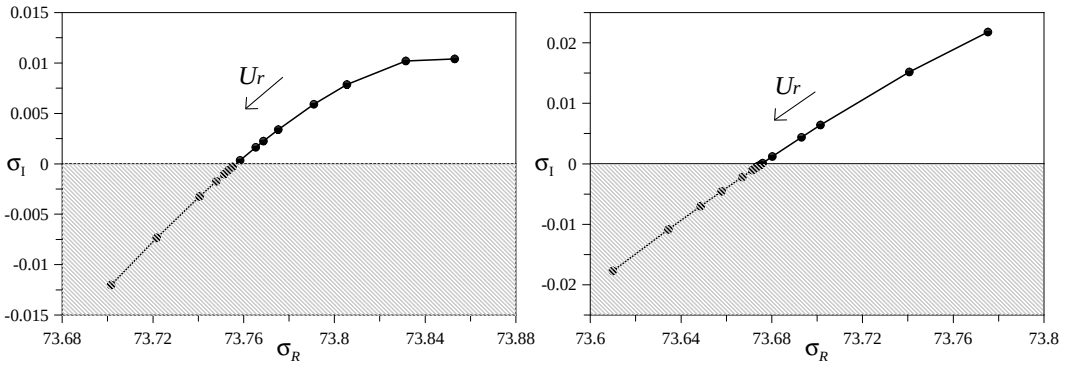

Figure 6: Flutter (grey zone) and stability (white zone) regions, undamped (left) and damped (right), when the wind angle of attack is $\alpha = +3^\circ$ and the bridge is pre-stressed by the dead loads.

	Undamped				$\zeta_u = \zeta_\phi = 0.5\%$			
α	$U_{r,c}$	$f_c[Hz]$	$U_c[m/s]$	$U_c[km/h]$	$U_{r,c}$	$f_c[Hz]$	$U_c[m/s]$	$U_c[km/h]$
Wind tunnel experimental results								
0°	> 16.3				> 16.3			
$+3^\circ$	3.61	0.66	46.7	168.12	4.21	0.65	53.4	192.24
Continuum nonlinear model results								
0°	> 16.3				> 16.3			
$+3^\circ$	3.29	0.729	47.18	169.85	4.275	0.728	60.68	218.45
Continuum nonlinear model results, pre-stress contribution								
0°	> 16.3				> 16.3			
$+3^\circ$	3.275	0.689	43.97	158.31	4.305	0.688	57.74	207.86

Table 2: Critical wind velocity at the onset of flutter.

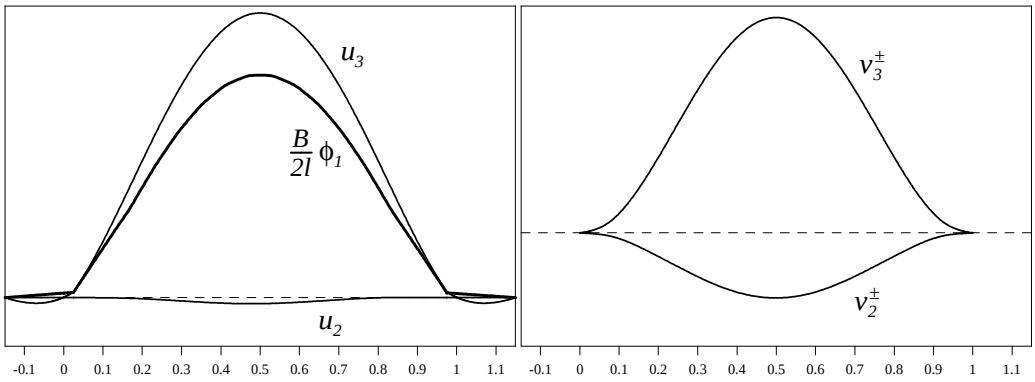

Figure 7: *Ponte della Musica*: flutter mode shape (frequency $f = 0.729$ Hz), deck (left) and arches (right).

5 CONCLUSIONS

A parametric nonlinear model of arch bridges has been proposed employing a geometrically exact formulation for the arches and the bridge deck. The obtained nonlinear equations of motion have been solved via a PDE-mode finite element discretization considering the Roman arch bridge named *Ponte della Musica*.

A preliminary modal analysis has been carried out considering the proposed parametric model and by comparing the outcomes with the results obtained employing directly the linear FE structural model used for the design. Subsequent to the evaluation of the pre-stressed condition induced by the dead loads, a nonlinear load path has been calculated by increasing the vehicles and pedestrian load multiplier. In particular, the multiplier that leads to the loss of the elastic stability has been determined. Then, the complex-valued eigenvalue problem has been set up and solved to calculate the onset of flutter. In this evaluation, the effects of the pre-stressed state due to the in-service loads were taken into account. The adopted bridge flutter derivatives were experimentally obtained for different wind angles of attack at the CRIACIV Laboratory in Prato.

The eigenvalue analysis has been conducted for the case of the undamped structure and for the standard damping ratio of 0.5%. In the undamped case, by considering the equations linearized about the stress-free configuration, a close agreement has been found with the experimental wind tunnel measurements for an angle of attack $\alpha = +3°$, with differences of the order of 1%. The fully nonlinear character of the proposed parametric structural model has allowed a more refined computation that accounts for the negative stiffness induced in the bridge pre-stressed state by the dead loads. This condition is not considered in the experimental tests. The evaluated critical wind velocity turns out to be 7% lower than the flutter speed of the stress-free structure. On the other hand, consideration of damping in the balance equations results into an expected increase of the flutter velocity with respect to the undamped case.

The proposed continuum model proved to be a reliable parametric nonlinear model that allows various types of nonlinear analysis as well as linearized structural analysis leading to the determination of various static and aeroelastic limit states towards the assessment of the bridge safety and comfort characteristics.

References

[1] Wen, R.K. and Medallah, K., "Elastic stability of deck-type arch bridges," *Journal of Structural Engineering, ASCE*, **113(4)**, 757-768 (1987).

[2] Nazmy, A.S., "Stability and load-carrying capacity of three-dimensional long-span steel arch bridges," *Computers and Structures*, **65(6)**, 857–868 (1997).

[3] Komatsu, S. and Sakimoto, T., "Ultimate load carrying capacity of steel arches," *Journal of the Structural Division, ASCE*, **103 (12)**, 2323-2336 (1977).

[4] Lacarbonara, W. and Arena, A., "Aerostatic torsional divergence of suspension bridges via a fully nonlinear continuum formulation," in *Atti di 10^{mo} Convegno Nazionale di Ingegneria del Vento, IN-VENTO 2008, Cefalù (PA), giugno 8-11, 2008*.

[5] Lacarbonara, W. and A. Arena, A., "Three-dimensional model of suspension bridges via a fully nonlinear continuum formulation," in *Atti di GIMC 2008, XVII Convegno Italiano di Meccanica Computazionale, Alghero, settembre 10-12, 2008*.

[6] Simiu, E. and Scanlan, R., *Wind effects on structures-Fundamentals and Applications to Design*, Third Edition, *Wiley-Interscience Publication*, (1996).

[7] Petrini, F., Giuliano, F. and Bontempi, F., "Comparison of time domain techniques for the evaluation of the response and the stability in long span suspension bridges," *Computers and Structures*, **85**, 1032-1048 (2007).

[8] Scanlan, R.H., "Reexamination of sectional aerodynamic force functions for bridges," *Journal of Wind Engineering and Industrial Aerodynamics*, **89**, 1257–1266 (2001).

[9] M.P. Petrangeli & Associati, "*Ponte della Musica*: Verifica delle strutture in acciaio dell'arco, dell'impalcato e della soletta," codifica E281004300SXA, (2008).

[10] Antman, S.S., *Nonlinear problems of elasticity*, 2nd ed. New York: Springer-Verlag, (2005).

[11] "UNI EN 1991-1-7: Part 1-7: Azioni in generale - Azioni eccezionali," (2006).

[12] "UNI EN 1991-2: Part 2: Carichi da traffico sui ponti," (2005).

[13] Theodorsen, T., "General theory of aerodynamic instability and the mechanism of flutter," *JNACA REPORT No. 496*, 291–311 (1935).

[14] Augusti, G., Spinelli, P., Borri, C., Bartoli, G., Giachi, M. and Giordano, S., "The C.R.I.A.C.I.V. Atmospheric Boundary Layer Wind Tunnel," in *Wind Engineering : retrospect and prospect, IAWE, International Association for Wind Engineering*, vol. 5, Wiley Eastern Limited, New Delhi (1995).

[15] Sarkar, P.P., Caracoglia, L., Haan, F.L. Jr., Sato, H., Murakoshid, J., "Comparative and sensitivity study of flutter derivatives of selected bridge deck sections, Part 1: Analysis of inter-laboratory experimental data," *Engineering Structures*, **31**, 158–169 (2009).